Experimental Investigation of Concrete Fatigue Resistance




Eng. Sara Korte[1]
Scientific researcher
Sara.Korte@UGent.be

Veerle Boel[1]
Prof. Dr. Eng.
Veerle.Boel@UGent.be

Wouter De Corte[1]
Prof. Dr. Eng.
Wouter.DeCorte@UGent.be

Geert De Schutter[2]
Prof. Dr. Eng.
Geert.DeSchutter@UGent.be

[1]Ghent University
Faculty of Engineering and Architecture
Dept. of Industrial Technology & Construction
Valentin Vaerwyckweg 1, B-9000 Ghent

[2]Ghent University
Faculty of Engineering and Architecture
Dept. of Structural Engineering
Technologiepark 904, B-9052 Zwijnaarde

ABSTRACT
A lack of knowledge on the fatigue resistance of self-compacting concrete (SCC) structures has led to the research presented in this paper. Several reinforced concrete beams were subjected to both static and cyclic four-point bending tests in order to determine the failure mechanism, the static ultimate load, the fatigue performance, the deformation, and crack width evolution. For comparison purpose, different mixtures were considered, including a vibrated concrete (VC) type and two SCCs (one with similar strength and one with equal w/c ratio, compared to VC). The mutual relationship is strongly depending on the stress level caused by the repeated loading.

Keywords: Vibrated Concrete, Self-compacting Concrete, Reinforcement, Fatigue, Cracking

1. INTRODUCTION
The different composition of SCC, compared to VC, influences various material characteristics, such as the microstructure, the interfacial transition zone, the compressive and tensile strength, the stiffness, and also the fracture behaviour. Therefore, it is assumed that the fatigue resistance of both concrete types might be different, since it is governed by a damage process, related to micro-crack initiation, material damage, and fracture behaviour in general.

2. EXPERIMENTAL PROGRAM
2.1 Mixtures
Three concrete batches were used: one vibrated concrete (VC) and two self-compacting concretes (SCC1 with similar strength and SCC2 with equal w/c ratio of 0.45). Table 1 and 2 provide the composition quantities of the mixtures, and their main properties.

2.2 Specimens
Aiming for concrete crushing at ultimate load with the steel rebar deformation remaining fully elastic, the 2.40m long beams were over-reinforced by using three longitudinal bars Ø20mm at

the bottom, two longitudinal bars Ø6mm at the top, and vertical stirrups Ø6mm every 55mm (Fig. 1). In addition, the upper part of the geometrical section is narrowed, thus generating larger concrete compressive bending stresses than there would occur in case of a rectangular section.

Table 1 – Concrete compositions

Composition	VC [kg/m³]	SCC1 [kg/m³]	SCC2 [kg/m³]
CEM III/A 42.5 LA	360	293	360
Water	161	161	161
Sand 0/4	759	651	651
Crushed limestone 2/6.3	433	523	523
Crushed limestone 6.3/14	610	321	321
Limestone filler	-	377	317
Superplasticizer (PCE)	2.7	9	9.5

Table 2 – Concrete hardened properties

Properties	VC [MPa]	SCC1 [MPa]	SCC2 [MPa]
f_{cm}	53.4	51.3	60.0
$f_{c,cub,m}$	54.3	53.9	63.8
$f_{ck} = f_{cm} - 1.64s$*	45.4	43.3	52.0
$f_{c,cub,k} = f_{c,cub,m} - 1.64s$*	46.3	45.9	55.8
$f_{ctm} = 0.3\ f_{ck}^{2/3}$	3.8	3.7	4.2
E_{cm}	38,423	38,093	35,290

**s = standard deviation*

2.3 Test procedure

Fig. 2 depicts the four-point bending test setup, applied for both static and fatigue tests. During all the experiments, the structural behaviour of the beams was registered by means of three strain gauges (n°1 in the middle of the top surface, n°2 along the side of the beam at 5cm from the top, n°3 at the lower side of the middle rebar) and three deflection gauges (at midspan and below the point loads). The crack width evolution was measured using a crack width microscope with an accuracy of 20µm. Three reference beams per concrete type were tested statically, with increments of 5kN up until failure, in order to determine the failure mechanism and the ultimate load P_{ult}. The cyclic tests then were conducted by applying a sinusoidal load function with a frequency of 1Hz and a lower limit of 10%P_{ult} and upper limits of 60%, 70%, 80%, and 85%P_{ult}.

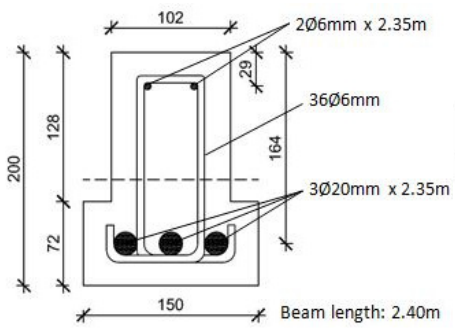

Fig. 1 – Concrete beam cross section

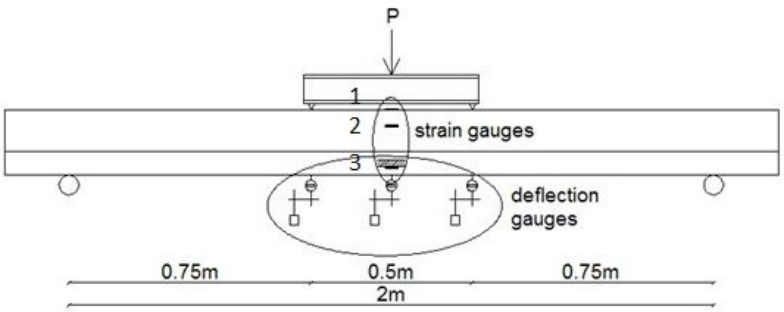

Fig. 2 – Test setup

3. RESULTS AND DISCUSSION

3.1 Static tests

All nine reference beams failed by pure concrete crushing. The average ultimate load was 132kN for VC, 162kN for SCC1, and 158kN for SCC2. The higher value for SCC2 is not surprising, given its higher compressive strength, but SCC1, which has a compressive strength similar to VC, can also resist a substantially higher load. As regards the average experimental midspan deflection, the measurements reveal smaller values for the SCC types. The difference with VC is minimal at the beginning of the static test, but increases towards failure. At a common load of 120kN the deviation with respect to VC is 17% in case of SCC1 and 14% in case of SCC2. Since VC has the smallest failure load, its larger deflection could be expected. Despite this, the crack width progression demonstrates a larger amount of cracks and consequently a more dense crack pattern for SCC (especially SCC1), compared to VC. The crack widths of SCC1 are up to 16% smaller than those of VC and up to 33% smaller than in case of SCC2. When considering the concrete strain evolution, corresponding values are noticed for both SCCs, which are exceeded by the concrete strain in VC with approximately 28% (near

the point of collapse). The ultimate strain values confirm the concrete crushing failure mode, for the strain failure limit of 3.5‰ is (practically) reached for all concrete types. From the results of the strain measurements on the reinforcement steel, the linear evolution ascertains that no plastic rebar deformation occurred during the loading process.

3.2 Fatigue tests

Table 3 lists the number of cycles to failure and the failure mode of the cyclic tests. It can be seen that the beams, subjected to the loading intervals 10-80 and 10-85 fail by crushing of the concrete in the compression zone, whereas for the lower upper limits the larger number of cycles causes rebar fatigue damage, developing more quickly than the deterioration process in the compressed concrete takes place. Specimen SCC1(10-70) is an exception, but examination of the reinforcement steel after collapse visibly demonstrated fatigue crack initiation. Despite some scatter, it is clear that the fatigue life depends on the applied load level: the higher the upper load limit, the least cycles the beams can sustain. When comparing SCC to VC, it could be stated that VC performs best in the fatigue tests with lower load levels (10-70, 10-60), which corresponds with the lower fatigue resistance of SCC, mentioned in Model Code 2010, due to the higher paste content and the different pore structure. The higher loading ranges, however, yield an opposite relationship: the longest fatigue life occurs for SCC1 (10-85) or SCC2 (10-80).

Table 3 – Number of cycles to failure

	VC		SCC1		SCC2	
Load level	# cycles	Failure mode	# cycles	Failure mode	# cycles	Failure mode
10-85% P_{ult}	5	CC	9,837	CC	992	CC
10-80% P_{ult}	17,812	CC	16,402	CC	126,443	CC
10-70% P_{ult}	290,598	RF	206,989	CC	234,500	RF
10-60% P_{ult}	1,050,056	RF	378,618	RF	339,551	RF

When considering the deformation evolution during the fatigue experiments, similar curves are found for the vertical displacement and strain measurements. First, a long period of slightly increasing deformation is present, followed by a rapid growth up to failure. Again, the loading range is crucial: the initial (and ultimate) value increases as the upper load limit increases. The relationship between the three concrete types is not unique, but also depends on the loading interval. In case of the lowest levels (10-70, 10-60), where most of the specimens failed by rebar fatigue and where VC showed the longest fatigue life, the deflection of VC is consistently smaller than that of the SCC mixtures. The other load levels (10-85, 10-80) indicate a larger deviation. The highest value occurs for SCC1, followed by VC and SCC2, respectively. However, there is no link with the number of cycles to failure. In contrast to these findings, the concrete strain data do not reveal an explicit relationship between VC and SCC regarding the magnitude of the strain values, even though a faster strain increase is noticed in case of SCC. Furthermore, it is observed that none of the specimens – not even those which collapsed by crushing of the concrete – achieves the 3.5‰ strain limit, which can be attributed to the redistribution process of the compressive stresses from the most degraded top fibres towards the lower and less damaged fibres in the compression zone (Zanuy et al. 2007). The rebar strain development shows nearly horizontal curves for all specimens far below the threshold value for yielding, pointing out merely elastic cross-sectional deformations. As regards the crack patterns, drawn during the cyclic tests, no substantial differences appear between the initial crack lengths (at the beginning of the experiment) and the ultimate crack lengths (at the end of the fatigue life). The crack widths do increase significantly as a function of the number of cycles. Depending on the loading range, the curves have an initial crack width between 0.1mm and 0.2mm. The gradual increase is quite similar for all concrete types, but the crack growth takes place at an accelerated level for the SCC mixtures, especially in case of the highest loading

intervals. This may be explained by the better bond properties of SCC, which induce significantly larger rebar stresses at the cracks, opposed to at the bar lengths between the cracks (Zanuy et al. 2011). Minimal differences in crack width values occur for the load levels 10-60 and 10-80, whereas in case of the other load limits SCC1 shows the largest crack widths, followed by VC and SCC2, respectively. Strangely, no correspondence is present with the rebar strain evolution. Observing the number of cracks, SCC1 and particularly SCC2 seems to produce more cracks, compared to VC. This phenomenon might be ascribed to the development of negative tension stiffening (negative bond stresses at the steel-concrete interface between cracks) during unloading stages, as it is observed by Zanuy et al. (Zanuy et al. 2011).

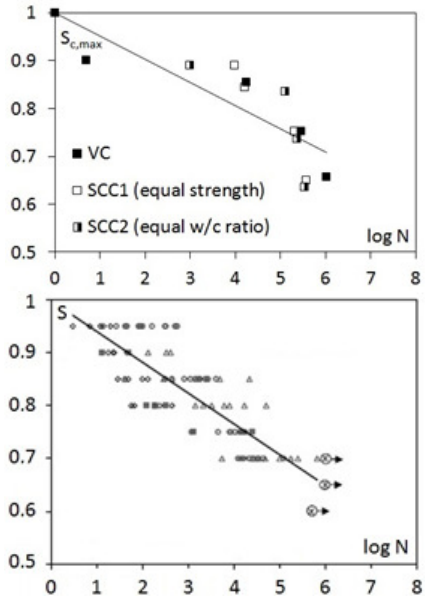

Based on the experimental fatigue data, the S-N curves in Fig. 3a represent the relationship between the maximum applied fatigue stress $\sigma_{c,max}$ (determined by using a nonlinear calculation method) and the number of load cycles N which cause fatigue failure. Relating $\sigma_{c,max}$ to the ultimate static concrete crushing stress f_{cc} yields the dimensionless term S, thus partly eliminating influences such as w/c ratio, moisture content, age at loading, etc. (Lee & Barr, 2004). A gently descending curve with similar slopes can be noticed for the three concrete types, which means that, when a certain fatigue stress level is applied, VC, SCC1 and SCC2 are able to endure an equal number of loading cycles before failing. Comparison of the outcome with Fig. 3b for plain concrete under repeated compressive loading (Lee & Barr, 2004), reveals good agreement.

Fig. 3 – S-N curve – a) experiments – b) Lee & Barr, 2004

4. CONCLUSIONS

During the cyclic tests, VC and SCC demonstrate a similar deformation evolution, but the values are larger for SCC in case of the highest applied load levels (10-80% and 10-85% of the static failure load). Furthermore, SCC (especially SCC2 with equal w/c ratio, with respect to VC) generates, on average, a larger amount of cracks in these loading intervals, and the fatigue crack propagation also takes place at an accelerated level. Strangely, SCC1 (with similar strength, compared to VC) shows the best fatigue resistance at the 10-85 range and SCC2 at the 10-80 interval, whereas VC shows the best fatigue resistance in case of the lower loading levels. No consistent relationship, covering the full loading scope, can be observed. The S-N curves point out that the studied concrete types do not have a remarkably different fatigue behaviour, since almost identical slopes are found.

REFERENCES

Lee, M.K., Barr, B.I.G., 2004
"An overview of the fatigue behaviour of plain and fibre reinforced concrete", Cement & Concrete Composites, Vol. 26, 2004, pp. 299-305.

Zanuy, C., de la Fuente, P., Albajar, L., 2007
"Effect of fatigue degradation in the compression zone of concrete in reinforced concrete sections", Engineering Structures, Vol. 29, 2007, pp. 2908-2920.

Zanuy, C., Maya, L.F., Albajar, L., de la Fuente, P., 2011
"Transverse fatigue behaviour of lightly reinforced concrete bridge decks", Engineering Structures, Vol. 33, 2011, pp. 2839-28-49.